



Fermi National Accelerator Laboratory

FERMILAB-Pub-92/286-E

**Comparison of Jet Production in $\bar{p}p$ Collisions at
 $\sqrt{s} = 546$ and 1800 GeV**

**F. Abe et al
The CDF Collaboration**

Fermi National Accelerator Laboratory, Batavia, Illinois 60510

October 1992

Submitted to *Physical Review Letters*



Operated by Universities Research Association Inc. under Contract No. DE-AC02-76CHO3000 with the United States Department of Energy

Disclaimer

This report was prepared as an account of work sponsored by an agency of the United States Government. Neither the United States Government nor any agency thereof, nor any of their employees, makes any warranty, express or implied, or assumes any legal liability or responsibility for the accuracy, completeness, or usefulness of any information, apparatus, product, or process disclosed, or represents that its use would not infringe privately owned rights. Reference herein to any specific commercial product, process, or service by trade name, trademark, manufacturer, or otherwise, does not necessarily constitute or imply its endorsement, recommendation, or favoring by the United States Government or any agency thereof. The views and opinions of authors expressed herein do not necessarily state or reflect those of the United States Government or any agency thereof.

Comparison of Jet Production in $\bar{p}p$ Collisions at $\sqrt{s} = 546$ and 1800 GeV

F. Abe,⁽¹¹⁾ D. Amidei,⁽¹⁴⁾ C. Anway-Wiese,⁽³⁾ G. Apollinari,⁽²⁰⁾ M. Atac,⁽⁶⁾ P. Auchincloss,⁽¹⁹⁾
P. Azzi,⁽¹⁵⁾ A. R. Baden,⁽⁸⁾ N. Bacchetta,⁽¹⁵⁾ W. Badgett,⁽¹⁴⁾ M. W. Bailey,⁽¹⁸⁾ A. Bamberger,^(6,a)
P. de Barbaro,⁽¹⁹⁾ A. Barbaro-Galtieri,⁽¹²⁾ V. E. Barnes,⁽¹⁸⁾ B. A. Barnett,⁽¹⁰⁾ G. Bauer,⁽¹³⁾
T. Baumann,⁽⁸⁾ F. Bedeschi,⁽¹⁷⁾ S. Behrends,⁽²⁾ S. Belforte,⁽¹⁷⁾ G. Bellettini,⁽¹⁷⁾ J. Bellinger,⁽²⁵⁾
D. Benjamin,⁽²⁴⁾ J. Benlloch,^(6,a) J. Bensinger,⁽²⁾ A. Beretvas,⁽⁶⁾ J. P. Berge,⁽⁶⁾ S. Bertolucci,⁽⁷⁾
K. Biery,^(16,a) S. Bhadra,⁽⁹⁾ M. Binkley,⁽⁶⁾ D. Bisello,⁽¹⁵⁾ R. Blair,⁽¹⁾ C. Blocker,⁽²⁾ A. Bodek,⁽¹⁹⁾
V. Bolognesi,⁽¹⁷⁾ A. W. Booth,⁽⁶⁾ C. Boswell,⁽¹⁰⁾ G. Brandenburg,⁽⁸⁾ D. Brown,⁽⁸⁾ E. Buckley-
Geer,⁽²¹⁾ H. S. Budd,⁽¹⁹⁾ G. Busetto,⁽¹⁵⁾ A. Byon-Wagner,⁽⁶⁾ K. L. Byrum,⁽²⁵⁾ C. Campagnari,⁽⁶⁾
M. Campbell,⁽¹⁴⁾ A. Caner,⁽⁶⁾ R. Carey,⁽⁸⁾ W. Carithers,⁽¹²⁾ D. Carlsmith,⁽²⁵⁾ J. T. Carroll,⁽⁶⁾
R. Cashmore,^(6,a) A. Castro,⁽¹⁵⁾ F. Cervelli,⁽¹⁷⁾ K. Chadwick,⁽⁶⁾ J. Chapman,⁽¹⁴⁾ G. Chiarelli,⁽⁷⁾
W. Chinowsky,⁽¹²⁾ S. Cihangir,⁽⁶⁾ A. G. Clark,⁽⁶⁾ M. Cobal,⁽¹⁷⁾ D. Connor,⁽¹⁶⁾ M. Contreras,⁽⁴⁾
J. Cooper,⁽⁶⁾ M. Cordelli,⁽⁷⁾ D. Crane,⁽⁶⁾ J. D. Cunningham,⁽²⁾ C. Day,⁽⁶⁾ F. DeJongh,⁽⁶⁾
S. Dell'Agnello,⁽¹⁷⁾ M. Dell'Orso,⁽¹⁷⁾ L. Demortier,⁽²⁾ B. Denby,⁽⁶⁾ P. F. Derwent,⁽¹⁴⁾ T. Devlin,⁽²¹⁾
D. DiBitonto,⁽²²⁾ M. Dickson,⁽²⁰⁾ R. B. Drucker,⁽¹²⁾ K. Einsweiler,⁽¹²⁾ J. E. Elias,⁽⁶⁾ R. Ely,⁽¹²⁾
S. Eno,⁽⁴⁾ S. Errede,⁽⁹⁾ A. Etchegoyen,^(6,a) B. Farhat,⁽¹³⁾ G. J. Feldman,⁽⁸⁾ B. Flaughner,⁽⁶⁾
G. W. Foster,⁽⁶⁾ M. Franklin,⁽⁸⁾ J. Freeman,⁽⁶⁾ H. Frisch,⁽⁴⁾ T. Fuess,⁽⁶⁾ Y. Fukui,⁽¹¹⁾
A. F. Garfinkel,⁽¹⁸⁾ A. Gauthier,⁽⁹⁾ S. Geer,⁽⁶⁾ D. W. Gerdes,⁽⁴⁾ P. Giannetti,⁽¹⁷⁾ N. Giokaris,⁽²⁰⁾
P. Giromini,⁽⁷⁾ L. Gladney,⁽¹⁶⁾ M. Gold,⁽¹²⁾ J. Gonzalez,⁽¹⁶⁾ K. Goulianos,⁽²⁰⁾ H. Grassmann,⁽¹⁵⁾
G. M. Grieco,⁽¹⁷⁾ R. Grindley,^(16,a) C. Grosso-Pilcher,⁽⁴⁾ C. Haber,⁽¹²⁾ S. R. Hahn,⁽⁶⁾ R. Handler,⁽²⁵⁾
Submitted to Physical Review Letters October 19, 1992.

K. Hara,⁽²³⁾ B. Harral,⁽¹⁶⁾ R. M. Harris,⁽⁶⁾ S. A. Hauger,⁽⁵⁾ J. Hauser,⁽³⁾ C. Hawk,⁽²¹⁾ T. Hessing,⁽²²⁾
 R. Hollebeek,⁽¹⁶⁾ S. Hong,⁽¹⁴⁾ G. Houk,⁽¹⁶⁾ P. Hu,⁽²¹⁾ B. Hubbard,⁽¹²⁾ B. T. Huffman,⁽¹⁸⁾
 R. Hughes,⁽¹⁶⁾ P. Hurst,⁽⁸⁾ J. Huth,⁽⁶⁾ J. Hylen,⁽⁶⁾ M. Incagli,⁽¹⁷⁾ T. Ino,⁽²³⁾ H. Iso,⁽²³⁾ H. Jensen,⁽⁶⁾
 C. P. Jessop,⁽⁸⁾ R. P. Johnson,⁽⁶⁾ U. Joshi,⁽⁶⁾ R. W. Kadel,⁽¹²⁾ T. Kamon,⁽²²⁾ S. Kanda,⁽²³⁾
 D. A. Kardelis,⁽⁹⁾ I. Karliner,⁽⁹⁾ E. Kearns,⁽⁸⁾ L. Keeble,⁽²²⁾ R. Kephart,⁽⁶⁾ P. Kesten,⁽²⁾
 R. M. Keup,⁽⁹⁾ H. Keutelian,⁽⁹⁾ D. Kim,⁽⁶⁾ S. B. Kim,⁽¹⁴⁾ S. H. Kim,⁽²³⁾ Y. K. Kim,⁽¹²⁾ L. Kirsch,⁽²⁾
 K. Kondo,⁽²³⁾ J. Konigsberg,⁽⁸⁾ K. Kordas,^(16,a) E. Kovacs,⁽⁶⁾ M. Krasberg,⁽¹⁴⁾ S. E. Kuhlmann,⁽¹⁾
 E. Kuns,⁽²¹⁾ A. T. Laasanen,⁽¹⁸⁾ S. Lammel,⁽³⁾ J. I. Lamoureux,⁽²⁵⁾ S. Leone,⁽¹⁷⁾ J. D. Lewis,⁽⁶⁾
 W. Li,⁽¹⁾ P. Limon,⁽⁶⁾ M. Lindgren,⁽³⁾ T. M. Liss,⁽⁹⁾ N. Lockyer,⁽¹⁶⁾ M. Loreti,⁽¹⁵⁾ E. H. Low,⁽¹⁶⁾
 D. Lucchesi,⁽¹⁷⁾ C. B. Luchini,⁽⁹⁾ P. Lukens,⁽⁶⁾ P. Maas,⁽²⁵⁾ K. Maeshima,⁽⁶⁾ M. Mangano,⁽¹⁷⁾
 J. P. Marriner,⁽⁶⁾ M. Mariotti,⁽¹⁷⁾ R. Markeloff,⁽²⁶⁾ L. A. Markosky,⁽²⁶⁾ R. Mattingly,⁽²⁾
 P. McIntyre,⁽²²⁾ A. Menzione,⁽¹⁷⁾ E. Meschi,⁽¹⁷⁾ T. Meyer,⁽²²⁾ S. Mikamo,⁽¹¹⁾ M. Miller,⁽⁴⁾
 T. Mimashi,⁽²³⁾ S. Miscetti,⁽⁷⁾ M. Mishina,⁽¹¹⁾ S. Miyashita,⁽²³⁾ Y. Morita,⁽²³⁾ S. Moulding,⁽²⁾
 J. Mueller,⁽²¹⁾ A. Mukherjee,⁽⁶⁾ T. Muller,⁽³⁾ L. F. Nakae,⁽²⁾ I. Nakano,⁽²³⁾ C. Nelson,⁽⁶⁾
 D. Neuberger,⁽³⁾ C. Newman-Holmes,⁽⁹⁾ J. S. T. Ng,⁽⁸⁾ M. Ninomiya,⁽²³⁾ L. Nodulman,⁽¹⁾
 S. Ogawa,⁽²³⁾ R. Paoletti,⁽¹⁷⁾ V. Papadimitriou,⁽⁶⁾ A. Para,⁽⁶⁾ E. Pare,⁽⁸⁾ S. Park,⁽⁸⁾ J. Patrick,⁽⁶⁾
 G. Pauletta,⁽¹⁷⁾ L. Pescara,⁽¹⁵⁾ T. J. Phillips,⁽⁶⁾ F. Ptohos,⁽⁸⁾ R. Plunkett,⁽⁶⁾ L. Pondrom,⁽²⁵⁾
 J. Proudfoot,⁽¹⁾ G. Punzi,⁽¹⁷⁾ D. Quarrie,⁽⁶⁾ K. Ragan,^(16,a) G. Redlinger,⁽⁴⁾ J. Rhoades,⁽²⁵⁾
 M. Roach,⁽²⁴⁾ F. Rimondi,^(6,a) L. Ristori,⁽¹⁷⁾ W. J. Robertson,⁽⁵⁾ T. Rodrigo,⁽⁶⁾ T. Rohaly,⁽¹⁶⁾
 A. Roodman,⁽⁴⁾ W. K. Sakumoto,⁽¹⁹⁾ A. Sansoni,⁽⁷⁾ R. D. Sard,⁽⁹⁾ A. Savoy-Navarro,⁽⁶⁾
 V. Scarpine,⁽⁹⁾ P. Schlabach,⁽⁸⁾ E. E. Schmidt,⁽⁶⁾ O. Schneider,⁽¹²⁾ M. H. Schub,⁽¹⁸⁾ R. Schwitters,⁽⁸⁾

A. Scribano,⁽¹⁷⁾ S. Segler,⁽⁶⁾ Y. Seiya,⁽²³⁾ G. Sganos,^(16,a) M. Shapiro,⁽¹²⁾ N. M. Shaw,⁽¹⁸⁾
 M. Sheaff,⁽²⁵⁾ M. Shochet,⁽⁴⁾ J. Siegrist,⁽¹²⁾ A. Sill,⁽¹⁹⁾ P. Sinervo,^(16,a) J. Skarha,⁽¹⁰⁾ K. Sliwa,⁽²⁴⁾
 A. Spies,⁽¹⁰⁾ D. A. Smith,⁽¹⁷⁾ F. D. Snider,⁽¹⁰⁾ L. Song,⁽⁶⁾ T. Song,⁽¹⁴⁾ M. Spahn,⁽¹²⁾ P. Sphicas,⁽¹³⁾
 R. St. Denis,⁽⁸⁾ L. Stanco,^(6,a) A. Stefanini,⁽¹⁷⁾ G. Sullivan,⁽⁴⁾ K. Sumorok,⁽¹³⁾ R. L. Swartz, Jr.,⁽⁹⁾
 M. Takano,⁽²³⁾ K. Takikawa,⁽²³⁾ S. Tarem,⁽²⁾ F. Tartarelli,⁽¹⁷⁾ S. Tether,⁽¹³⁾ D. Theriot,⁽⁶⁾
 M. Timko,⁽²⁴⁾ P. Tipton,⁽¹⁹⁾ S. Tkaczyk,⁽⁶⁾ A. Tollestrup,⁽⁶⁾ J. Tonnison,⁽¹⁸⁾ W. Trischuk,⁽⁸⁾
 Y. Tsay,⁽⁴⁾ J. Tseng,⁽¹⁰⁾ N. Turini,⁽¹⁷⁾ F. Ukegawa,⁽²³⁾ D. Underwood,⁽¹⁾ S. Vejckik, III,⁽¹⁰⁾
 R. Vidal,⁽⁶⁾ R. G. Wagner,⁽¹⁾ R. L. Wagner,⁽⁶⁾ N. Wainer,⁽⁶⁾ R. C. Walker,⁽¹⁹⁾ J. Walsh,⁽¹⁶⁾
 G. Watts,⁽¹⁹⁾ T. Watts,⁽²¹⁾ R. Webb,⁽²²⁾ C. Wendt,⁽²⁵⁾ H. Wenzel,⁽¹⁷⁾ W. C. Wester, III,⁽¹²⁾
 T. Westhusing,⁽⁹⁾ S. N. White,⁽²⁰⁾ A. B. Wicklund,⁽¹⁾ E. Wicklund,⁽⁶⁾ H. H. Williams,⁽¹⁶⁾
 B. L. Winer,⁽¹⁹⁾ J. Wolinski,⁽²²⁾ D. Wu,⁽¹⁴⁾ J. Wyss,⁽¹⁵⁾ A. Yagil,⁽⁶⁾ K. Yasuoka,⁽²³⁾ Y. Ye,^(16,a)
 G. P. Yeh,⁽⁶⁾ C. Yi,⁽¹⁶⁾ J. Yoh,⁽⁶⁾ M. Yokoyama,⁽²³⁾ J. C. Yun,⁽⁶⁾ A. Zanetti,⁽¹⁷⁾ F. Zetti,⁽¹⁷⁾
 S. Zhang,⁽¹⁴⁾ W. Zhang,⁽¹⁶⁾ S. Zucchelli,^(6,a)

The CDF Collaboration

(1) *Argonne National Laboratory, Argonne, Illinois 60439*

(2) *Brandeis University, Waltham, Massachusetts 02254*

(3) *University of California at Los Angeles, Los Angeles, California 90024*

(4) *University of Chicago, Chicago, Illinois 60637*

(5) *Duke University, Durham, North Carolina 27706*

(6) *Fermi National Accelerator Laboratory, Batavia, Illinois 60510*

- (7) *Laboratori Nazionali di Frascati, Istituto Nazionale di Fisica Nucleare, Frascati, Italy*
- (8) *Harvard University, Cambridge, Massachusetts 02138*
- (9) *University of Illinois, Urbana, Illinois 61801*
- (10) *The Johns Hopkins University, Baltimore, Maryland 21218*
- (11) *National Laboratory for High Energy Physics (KEK), Japan*
- (12) *Lawrence Berkeley Laboratory, Berkeley, California 94720*
- (13) *Massachusetts Institute of Technology, Cambridge, Massachusetts 02139*
- (14) *University of Michigan, Ann Arbor, Michigan 48109*
- (15) *Universita di Padova, Istituto Nazionale di Fisica Nucleare, Sezione di Padova, I-35131 Padova, Italy*
- (16) *University of Pennsylvania, Philadelphia, Pennsylvania 19104*
- (17) *Istituto Nazionale di Fisica Nucleare, University and Scuola Normale Superiore of Pisa, I-56100 Pisa, Italy*
- (18) *Purdue University, West Lafayette, Indiana 47907*
- (19) *University of Rochester, Rochester, New York 14627*
- (20) *Rockefeller University, New York, New York 10021*
- (21) *Rutgers University, Piscataway, New Jersey 08854*
- (22) *Texas A&M University, College Station, Texas 77843*
- (23) *University of Tsukuba, Tsukuba, Ibaraki 305, Japan*
- (24) *Tufts University, Medford, Massachusetts 02155*
- (25) *University of Wisconsin, Madison, Wisconsin 53706*

Abstract

Inclusive jet cross-sections have been measured in $\bar{p}p$ collisions at $\sqrt{s} = 546$ and 1800 GeV,

using the CDF detector at the Fermilab Tevatron. The ratio of jet cross-sections is compared to predictions from simple scaling and $O(\alpha_s^3)$ QCD. Our data exclude scaling and lie $1.5\text{-}2.4\sigma$ below a range of QCD predictions.

PACS numbers: 13.87.-a, 12.38.Qk, 13.85.Ni

In this Letter we present a measurement of the scaling behavior of jet production at the Fermilab Tevatron $\bar{p}p$ Collider, using data taken with the CDF detector at two collision energies. The hypothesis of “scaling” predicts that jet production cross-sections, if scaled in a way that makes them dimensionless, will be independent of $\bar{p}p$ CM energy. By contrast, perturbative QCD calculations of parton hard scattering exhibit non-scaling behavior through the evolution of the proton structure functions and the running of the strong coupling constant, α_s . Although scaling violation in jet production at hadron colliders has been observed between CERN ISR and Sp \bar{p} S data [1], and ISR and Tevatron data [2], for the present measurement it has been possible to conduct the test within a single experiment, owing to the widely separated CM energies ($\sqrt{s} = 546$ and 1800 GeV) at which data were taken. This leads to substantially smaller systematic uncertainties, and a correspondingly more precise investigation into scaling behavior. We also note that in addition to providing a test of QCD predictions, the jet scaling measurement is important for extrapolating QCD event rates to LHC and SSC energies.

A detailed description of the CDF detector is given in Ref. [3]. The primary detector element used in this analysis is the central calorimeter, which subtends the pseudorapidity interval $|\eta| \leq 1.1$ ($\eta = -\ln(\tan(\theta/2))$), and spans 2π in azimuthal angle ϕ . Jet event triggering required one or more

clusters of energy within the calorimeter, defined in the trigger hardware, above a set of transverse energy (E_T) thresholds. E_T is defined with respect to the beam-line. Details of triggering, offline event selection, and background elimination for CDF inclusive central jet measurements are given in References [4] and [2]. The offline jet clustering algorithm, which defines jets based on calorimeter E_T within a cone of radius 0.7 in (η, ϕ) , is detailed in Ref. [5]. Jets in the offline analysis are restricted to the central rapidity interval ($0.1 \leq |\eta| \leq 0.7$).

Two inclusive jet data sets were used in this analysis: (1) the full 1988-89 run at $\sqrt{s}=1800$ GeV (integrated luminosity = 4.43 pb^{-1}), and (2) a short run at $\sqrt{s}=546$ GeV (8.58 nb^{-1}). To reduce systematics for comparing jet production in the two samples, the online triggering, offline analysis chain, and event selection criteria were identical and standard (see Ref. [4]), apart from the following set of requirements or corrections made to the 546 GeV data. (1) The E_T threshold for clusters in the trigger hardware was set to 15 GeV, and the clusters were restricted to the central calorimeter. We note that data taken at 1800 GeV with these two requirements were found to agree with standard jet trigger data from the full 1800 GeV run. (2) To compensate for the small size of the 546 GeV data sample, the cut on offline jet E_T was lowered to the point at which single offline jets pass the trigger with 90% efficiency ($E_T=25.7$ GeV). This necessitated a $< 10\%$ rate correction for jets with offline E_T below 33 GeV, where the trigger is fully efficient. (3) Event vertices in z , along the beam-line, were required to be within 60 cm of the detector center for both data sets; however, the efficiency of this cut was evaluated separately for the two sets to account for a 16% increase in width of the luminous region at 546 GeV. Approximately 1400 (40,300) jets in the 546 (1800) GeV sample pass all requirements.

The observed inclusive jet E_T spectra were corrected for energy loss and resolution effects. Corrections were obtained using a tuned Monte Carlo detector simulation described elsewhere [4]. Confirmation of our Monte Carlo modeling of jet losses and resolution has come from comparing data and Monte Carlo predictions for momentum balance in photon-jet and di-jet events in the 1800 GeV sample. Using Monte Carlo events, corrected jet E_T was defined as the sum of the E_T 's of all final state particles pointing within the clustering cone, excluding only particles originating from the underlying non-jet interaction. The average non-jet energy within the clustering cone was 0.9 (1.5) GeV at 546 (1800) GeV CM energy, defined as the observed calorimeter transverse energy at 90° to the jet axis in CDF di-jet events. Fluctuations in this energy, different for the two data samples, contribute to jet E_T resolution. No correction was made for jet E_T lost outside the clustering cone, in order to facilitate comparisons to next-to-leading order ($O(\alpha_s^3)$) calculations which depend explicitly on cone-size.

An iterative procedure was used to correct the measured cross-sections. For each data set, a function representing a test corrected cross-section was subjected to E_T loss and resolution effects, binned, and compared to the measured cross-section. The initial test cross-section was then iterated until a good match to the data was achieved. Corrections to the measured cross-section were obtained by comparing the resulting test cross-section to the data. Corrections to offline jet E_T compensate for the competing effects of losses and the “feed-up” of lower true E_T 's into higher offline E_T bins, and range in the 546 (1800) GeV data from 1.05 to 1.10 (1.07-1.09) over the corrected E_T interval 28-72 (40-415) GeV. Corrections to the measured rate in a given E_T bin range from 1.42 to 1.63 (1.19-1.21) over this same E_T interval.

Systematic uncertainty on the corrected cross-sections arises from the following sources: (1) knowledge of calorimeter energy response to hadrons and electron/photons, (2) modeling of jet resolution in the Monte Carlo, (3) Monte Carlo modeling of jet fragmentation, (4) non-jet energy correction, and (5) luminosity measurement. Other effects, such as any E_T dependence of the clustering algorithm, acceptance bias in the jet η distribution resulting from the trigger requirements, or uncertainty on the 546 GeV trigger efficiency correction, have been studied and are small ($< 5\%$). The uncertainty on non-jet energy for each data set is taken as $\pm_{50}^{30}\%$ of its value: the upper limit reflects a $\pm 30\%$ systematic uncertainty on the measurement of this energy in di-jet events, while the lower limit represents the level of transverse energy seen in a 0.7 cone in CDF minimum bias events, and thus accounts for possible jet contributions to the quantity we have defined as “non-jet energy”. Uncertainty on the jet E_T scale (Sources 1,3,&4) totals $+_{-3.8}^{4.5}\%$ ($+_{-1.6}^{2.6}\%$) for 25 (300) GeV jets. Absolute luminosity measurements have a 6.8% systematic uncertainty [6]. Overall systematic uncertainty on the 546 GeV inclusive central jet cross-section averaged over the central η interval, $\langle d\sigma/dE_T \rangle_\eta$, is $\pm_{26}^{23}\%$ in quadrature sum, nearly independent of E_T owing to the small E_T range subtended by the data. Sources 1-4 contribute roughly equally to this error. The 1800 GeV systematic uncertainty is $\pm 16\%$ for that part of the spectrum (91-238 GeV) which overlaps the 546 GeV data in the dimensionless energy variable $x_T (\equiv 2E_T/\sqrt{s})$, and is again nearly constant; sources 1,3,&4 are largest. The corrected 1800 GeV cross-section from this analysis is 12% below that of the analysis of the same data in Ref. [4], where a simpler version of the Monte Carlo-based corrections was used (accompanied by a correspondingly larger systematic uncertainty than the present measurement).

We note that the 546 GeV inclusive cross-section agrees well with previous measurements from the UA1 and UA2 experiments at the CERN Sp \bar{p} S Collider when similar definitions of corrected E_T are applied. Both CERN experiments defined jet corrections to give the E_T of the massless partons from the initial hard scattering, as predicted by their Monte Carlo event generators. This definition accounts for jet fragmentation energy lost outside the recognized jet cluster. To compare to CERN, CDF data were reprocessed using an analogous set of jet E_T corrections [7]. Figure 1 compares the corrected CDF jet cross-section at 546 GeV (both standard CDF data and ‘‘CERN-corrected’’ CDF data are shown) against UA2 results [1]. The data are also in good agreement with results from UA1 [8].

To test scaling behavior we form the ratio, R , of scaled invariant cross-sections ($E_T^4(E \frac{d^3\sigma}{dp^3})$), 546 GeV to 1800 GeV. These scaled cross-sections are dimensionless in natural units. The ratio was constructed bin-by-bin over the interval of x_T overlap, 0.101-0.265. Ratio data are tabulated in Table 1 along with the unscaled cross-sections, and are plotted in Fig. 2. Statistical uncertainties and a band of systematic uncertainty are also shown (for presentational purposes, this band has been centered on a fit to the ratio data). Because R represents the ratio of two jet cross-sections, with a common set of systematic uncertainties but over two ranges of jet E_T , correlations between the uncertainties of the two samples must be taken into account. To obtain the systematic uncertainty on R , the sources of error outlined above were varied one at a time for the two data sets, and the corrected cross-sections and ratio reevaluated; the deviation of the resulting ratios from the standard ratio defined the systematic uncertainties. The luminosity uncertainty on R is 4.6% [6]. The total systematic uncertainty is $\pm 16\%$ for the first x_T bin, and $\pm 13\%$ for the last bin; thus

about half of the systematic error on the individual cross-sections cancels in the ratio. For the first (last) x_T bin, the largest contributions are $\pm 6\%$ ($\pm 10\%$) from Source 1, $\pm 10\%$ ($\pm 4\%$) from Source 2, and $\pm 12\%$ ($\pm 3\%$) from Source 4.

The deviation of our ratio data from the scaling hypothesis prediction of unity was tested in two ways (in both tests we have taken systematic uncertainties to be Gaussian and have accounted for their bin-to-bin correlations). First, χ^2 was evaluated. A value of $\chi^2 = 14.3/11d.o.f.$ is found. However, because all points lie above the scaling prediction and χ^2 is insensitive to signs of deviations, we also compared the average value of R against unity. The average R for our data, constructed in a weighted fashion using statistical and systematic errors, is $1.51 \pm 0.04 \pm 0.21$. Comparing the data average to the scaling prediction yields a confidence level of 1.7%. We conclude that scaling in jet production is excluded by our data.

We have also compared our R data against next-to-leading order QCD calculations [9] for a variety of structure functions and choices of renormalization scale (Q^2). Figure 2 shows four such calculations. The roughly constant value above unity reflects structure function evolution, which depletes the 1800 GeV parton density in the x_T interval accessible to this measurement, and the lower value of α_s for 1800 GeV jet production at a given x_T relative to 546 GeV. Comparison to QCD predictions was made using the average-value technique, which again is more restrictive than χ^2 . Predictions for average R range from 1.83 to 2.01, and thus lie 1.5-2.4 σ above our data. Probability of agreement with our data improves as Q^2 increases in the calculations from $E_T^2/4$ to $4E_T^2$ (lowering the prediction for R), ranging from 3-12% for structure function set HMRS(B) [10], 3-13% for MTB and 2-9% for MTS [11]. Unlike predictions for the individual jet cross-sections, which vary by $\pm 7\%$

over the structure function range and $\pm 13\%$ over the Q^2 interval, predictions for R vary by only $\pm 1\%$ and $\pm 4\%$. The dependence of the calculations for R on Q^2 is illustrated in Fig. 2.

Also, for each structure function and Q^2 choice, comparison was made between N.L.O. QCD and jet cross-section data at 546 and 1800 GeV. Although experimental uncertainties are larger for the cross-sections than for the ratio, this test was conducted to ensure that, given a certain level of agreement with our ratio data, predictions for the individual cross-sections were at least consistent with our data. Using the χ^2 test evaluated over the 11 bins of E_T which correspond to the x_T bins of the scaling ratio, good agreement (probability $> 10\%$) was found for every N.L.O. prediction at both \sqrt{s} values. Figure 3 plots cross-section residuals with respect to a calculation using HMRSB; the effect of Q^2 scale choice on the QCD predictions is also shown.

The dependence of R on the jet clustering cone-size has been investigated by reevaluating our corrected cross-sections and ratio using a cone with radius 1.0. The cross-section ratio for cone=1.0 data agrees with cone=0.7 data to $\approx 5\%$; N.L.O. QCD predicts a 2% increase in R . We also note that $O(\alpha_s^2)$ and $O(\alpha_s^3)$ calculations for R are nearly identical, and that the HERWIG parton-shower Monte Carlo [12] predicts an R that lies $\approx 7\%$ above an N.L.O. calculation using the same structure functions. From the above, we conclude that the effects of higher order radiation and hadronization on R are less than 10%.

In summary, the ratio of dimensionless inclusive central jet cross-sections measured in CDF data at 546 and 1800 GeV has provided a test of QCD predictions with greater precision than that of the individual cross-sections; likewise, theoretical uncertainty is reduced by more than a factor

of three in the ratio. Unlike the cross-sections, the ratio is stable under changes in jet clustering radius. Using an average ratio test, our ratio data are inconsistent with scaling, and consistent at the 1.5-2.4 σ level with a range of next-to-leading order predictions, although our data favor a level for the ratio that is lower than that of the predictions tested.

We thank the Fermilab staff and the technical staffs of the participating institutions for their vital contributions. This work was supported by the U.S. Department of Energy and National Science Foundation, the Italian Istituto Nazionale di Fisica Nucleare, the Ministry of Science, Culture and Education of Japan, and the Alfred P. Sloan Foundation.

References

- [1] UA2 Collaboration, J. A. Appel *et al.*, Physics Letters B160, 349 (1985).
- [2] CDF Collaboration, F. Abe *et al.*, Phys. Rev. Lett., 62, 613 (1989).
- [3] CDF Collaboration, F. Abe *et al.*, Nucl. Instr. Meth. A 271, 387 (1988).
- [4] CDF Collaboration, F. Abe *et al.*, Phys. Rev. Lett., 68, 1104 (1992).
- [5] CDF Collaboration, F. Abe *et al.*, Phys. Rev. D 45, 1448 (1992).
- [6] CDF Collaboration, F. Abe *et al.*, Phys. Rev. D 44, 29 (1991).
- [7] The CERN E_T definition also introduces model-dependence through the unknown relationship of massless parton E_T to fragmented jet E_T . To make a more model-independent comparison

to CERN data, the CDF “CERN-like” jet E_T was defined as the sum of the E_T 's of *all final-state particles* associated with the initial parton, including those outside the clustering cone.

- [8] UA1 Collaboration, G. Arnison *et al.*, Phys. Lett. B172, 461 (1986).
- [9] S. Ellis, Z. Kunszt and D. Soper, Phys. Rev. Lett., 62, 2188 (1989); Phys. Rev. Lett., 64, 2121 (1990).
- [10] P. Harriman, A. Martin, R. Roberts and W. Stirling, Phys. Rev. D 43, 3648 (1991).
- [11] J. Morfin and W.K. Tung, Zeit. Phys. C 52, 13 (1991).
- [12] G. Marchesini and B.R. Webber, Nucl. Phys. B310, 461 (1988).

Figure 1: Inclusive jet cross-sections averaged over the central η interval, $\langle d\sigma/dE_T \rangle_\eta$, at $\sqrt{s}=546$ GeV. CDF data are shown with standard and “CERN-like” E_T corrections. Data from the UA2 experiment are also shown. CDF quadrature systematic uncertainty is shown in the key; UA2 points carry statistical and E_T -dependent systematic error, with normalization error in the key.

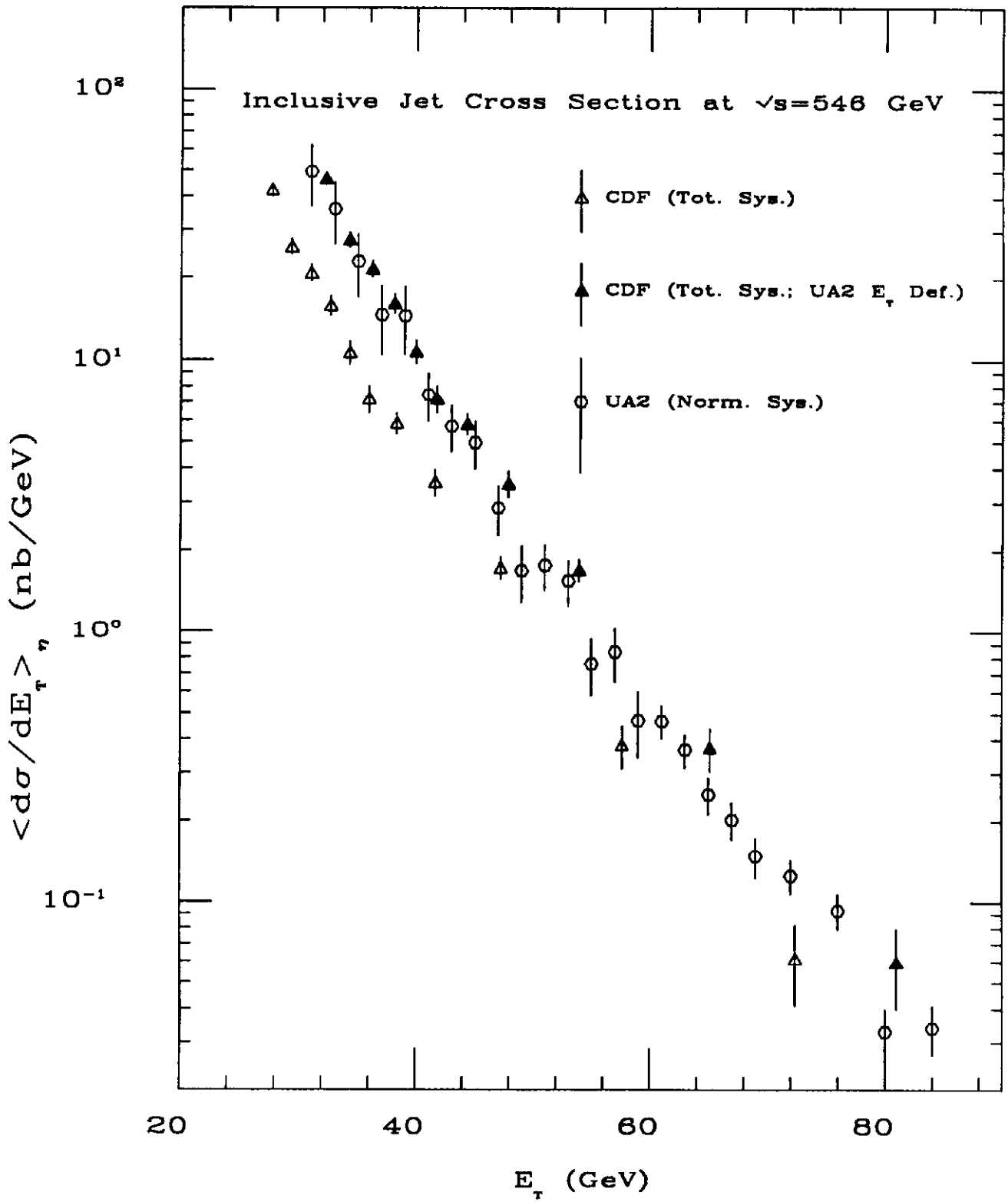
Figure 2: The ratio of 546 to 1800 GeV dimensionless jet cross-sections, R , vs. x_T . Statistical errors and a band of systematic error are shown. Four $O(\alpha_s^3)$ QCD calculations are also plotted, illustrating the variation with the choice of structure function and Q^2 scale.

Figure 3

Figure 3: Inclusive central jet cross-section residuals with respect to the HMRSB ($Q^2=E_T^2$) prediction, $(\text{Data-HMRSB})/\text{HMRSB}$. Data at $\sqrt{s}=546$ and 1800 GeV are shown. Systematic uncertainty is indicated in the key. The solid (dashed) line is the residual of an HMRSB calculation using $Q^2=4E_T^2$ against HMRSB with $Q^2=E_T^2$, at 1800 (546) GeV.

Table 1: CDF inclusive jet cross-section data at $\sqrt{s}=546$ and 1800 GeV, and the ratio of dimensionless cross-sections, as a function of x_T . Statistical errors are shown. Systematic uncertainty is $\pm\frac{23}{26}\%$ for 546 GeV data, $\pm 16\%$ for 1800 GeV data, and approximately ± 0.22 for the ratio.

x_T	$\langle d\sigma/dE_T \rangle_\eta^{546}$ (nb/GeV)	$\langle d\sigma/dE_T \rangle_\eta^{1800}$ (nb/GeV)	R
0.101	42.3 ± 2.3	$(8.47 \pm 0.33) \times 10^{-1}$	1.40 ± 0.10
0.107	26.0 ± 1.8	$(5.91 \pm 0.28) \times 10^{-1}$	1.23 ± 0.10
0.113	20.8 ± 1.5	$(4.37 \pm 0.24) \times 10^{-1}$	1.34 ± 0.12
0.119	15.7 ± 1.3	$(3.27 \pm 0.20) \times 10^{-1}$	1.35 ± 0.14
0.126	10.6 ± 1.0	$(2.223 \pm 0.032) \times 10^{-1}$	1.34 ± 0.13
0.132	7.20 ± 0.84	$(1.677 \pm 0.027) \times 10^{-1}$	1.21 ± 0.14
0.140	5.85 ± 0.53	$(1.085 \pm 0.016) \times 10^{-1}$	1.52 ± 0.14
0.152	3.56 ± 0.41	$(6.34 \pm 0.12) \times 10^{-2}$	1.58 ± 0.18
0.172	1.73 ± 0.17	$(2.836 \pm 0.048) \times 10^{-2}$	1.72 ± 0.17
0.211	0.380 ± 0.071	$(6.77 \pm 0.22) \times 10^{-3}$	1.58 ± 0.30
0.265	$0.062^{+0.028}_{-0.020}$	$(1.122 \pm 0.064) \times 10^{-3}$	$1.54^{+0.70}_{-0.50}$



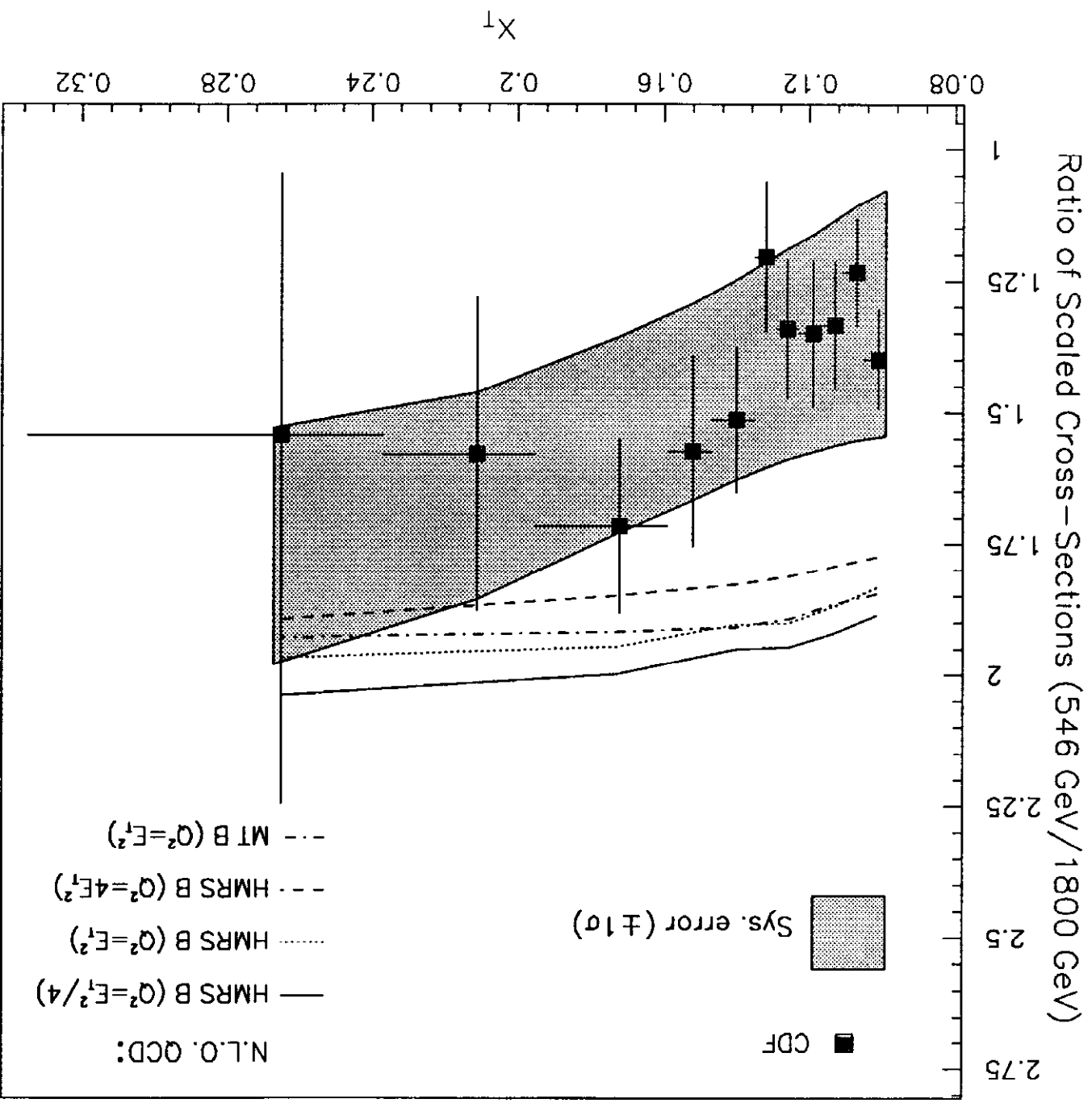


FIG. 2

Fractional Residual from Default Calculation

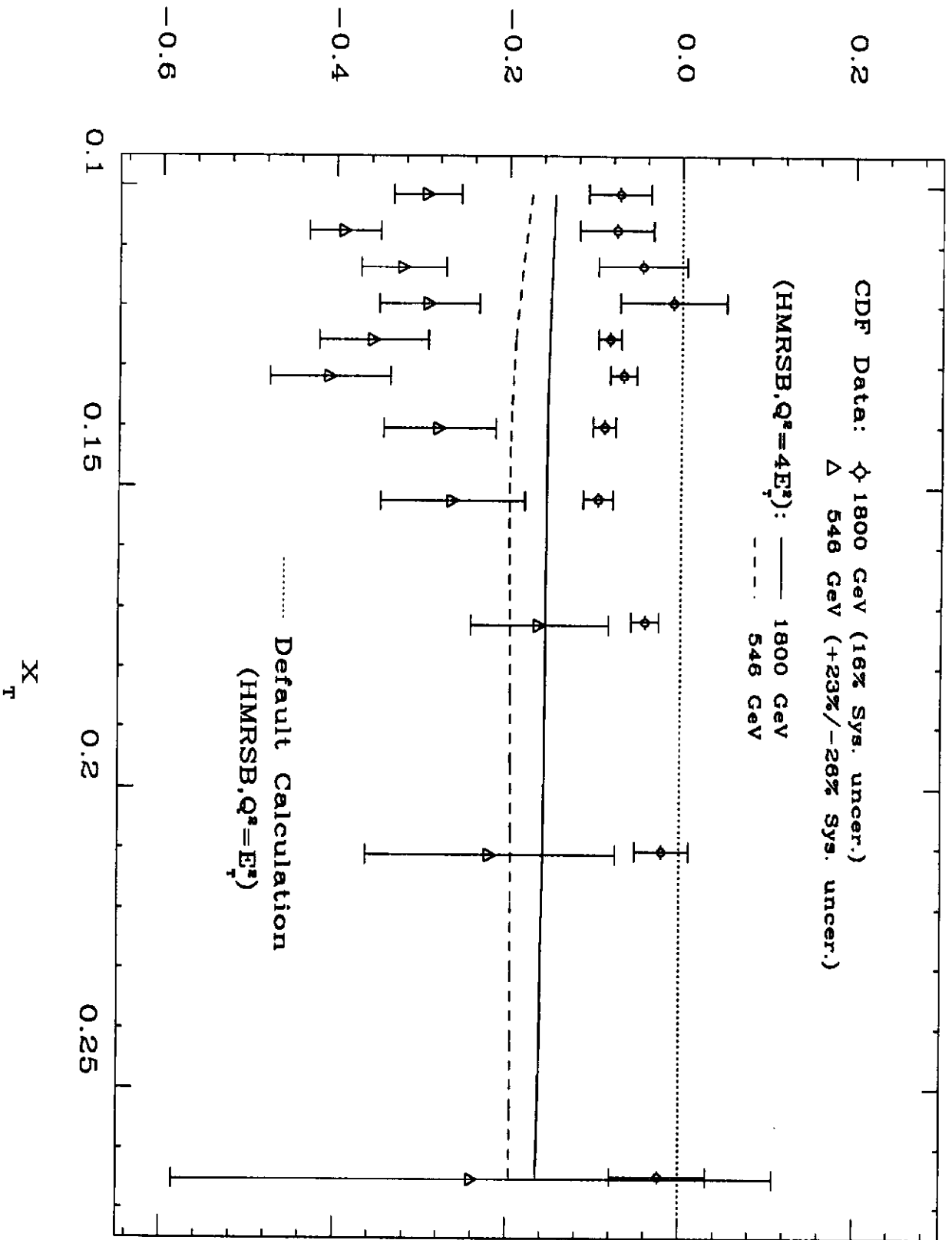


Fig. 3